

Magnetoelectric properties of oxygenated (Ga,Mn)AsL. Herrera Diez,^{*} M. Konuma, R. K. Kremer, J. Honolka, and K. Kern*Max-Planck-Institut für Festkörperforschung, Heisenbergstrasse 1, D-70569, Stuttgart, Germany*E. Placidi[†] and F. Arciprete*Dipartimento di Fisica, Università di Roma "Tor Vergata," and CNR-INFN, Via della Ricerca Scientifica 1, I-00133 Roma, Italy*

(Received 20 September 2010; revised manuscript received 27 January 2011; published 23 March 2011)

The effect of oxygen plasma exposure on the magnetoelectrical properties of (Ga,Mn)As films is investigated. A significant increase in the oxygen content of the plasma-treated (Ga,Mn)As is visible in depth-profile x-ray photoelectron spectroscopy. The temperature dependence of the electrical resistance shows that after oxygenation the (Ga,Mn)As films become more resistive and that the distinct peak accounting for the Curie temperature shifts to lower temperatures. In addition, larger coercive fields for all in-plane directions are observed in the magnetoresistance signal after the treatment. X-ray absorption spectroscopy evidences the preservation of the electronic d^5 state of the Mn atoms after oxygenation. This indicates that the changes in the electrical and consequently in the magnetic properties occur via a hole compensation mechanism promoted by the oxygen species incorporated during the plasma exposure.

DOI: [10.1103/PhysRevB.83.094420](https://doi.org/10.1103/PhysRevB.83.094420)

PACS number(s): 75.60.Ej, 75.50.Pp, 78.70.Dm, 79.60.Dp

Diluted magnetic semiconductors, especially (Ga,Mn)As,¹ are intensively studied since they are suitable materials for the development of novel applications in spintronics. Research has been focused not only on the development of devices exploiting the intriguing electrical and magnetic properties of this material but also on modifying the material itself, in order to add more degrees of freedom to control the magnetoelectric properties of (Ga,Mn)As. In this respect, a substantial improvement in view of practical applications was the achievement of higher Curie temperatures upon low-temperature annealing.²⁻⁴ On the other hand, methods allowing for the controlled suppression of ferromagnetism^{5,6} have been developed and can be important for devices where a local modification of the magnetic properties is required.

In this study we present the effect of oxygenation by oxygen plasma exposure on epitaxially grown (Ga,Mn)As. The general observation after the plasma treatment is a weaker ferromagnetic coupling, where the Curie temperature (T_c) shifts to lower values and the coercive field increases. These changes in the magnetic properties in addition to an increase in the electrical resistance point at a hole-quenching effect in agreement with the hole-mediated ferromagnetism present in (Ga,Mn)As.⁷ Using this oxygenation procedure, modifications of the magnetic properties can be achieved on a local scale. In this way, domain nucleation units can be produced for the controlled triggering of the magnetization reversal. Moreover, by this method these units could be generated in parallel at specific locations by the use of suitable masks, which is important for practical applications.

The (Ga,Mn)As samples used in this work were grown by molecular beam epitaxy (MBE) on a semi-insulating GaAs substrate.⁹ The manganese concentrations in the samples employed, designated *A* and *B*, are 1.2% and 3%, with thicknesses 170 and 40 nm, respectively. Magnetotransport measurements have been carried out using 30- μ m-wide Hall bar devices patterned along the hard $[1\bar{1}0]$ direction by standard photolithography. In the case of the oxygenated samples the oxygenation treatment was carried out after the Hall bar fabrication. The plasma treatment was performed

using a microwave (2450 MHz) TePla 100-E oxygen plasma system. By the use of a microwave plasma the surface charging during the treatment can be reduced to a minimum during the exposure compared to radio frequency plasmas used in hydrogenation experiments.⁶ Under these conditions of minimum charging there is only a negligible acceleration of ions toward the surface, which prevents undesired surface bombardment,⁸ leaving the films less damaged by the treatment. The results shown in this study were obtained from as-grown and oxygenated samples with an exposure time of 3 h (300 W input power, 1 mbar oxygen pressure). During plasma exposure the temperature of the samples was 177 °C. The depth profile of the x-ray photoelectron spectra (XPS) of sample *A* showing the oxygen content as a function of the distance from the surface for the as-grown (top) and oxygenated (bottom) samples is shown in Fig. 1. The oxygen content is represented by the peak area of the background subtracted O 1s peak in counts per second (CPS). The depth profile was acquired by recording the O 1s XPS spectrum between steps of sputtering with Ar⁺ ions accelerated at a voltage of 4 kV with an etching rate of 4.5 nm per minute. The presence of oxygen can already be detected in the as-grown sample, which is consistent with studies in the literature that report the formation of a manganese-rich surface oxide on (Ga,Mn)As exposed to air, which has been identified to be MnO.¹⁰ Additionally, Ga and As oxides known to form at the surface of GaAs materials in contact with air also contribute to the oxygen signal in (Ga,Mn)As films.¹¹ Although the surface oxide layer thickness in (Ga,Mn)As is reported to be between 1 and 2 nm,^{11,12} in our experiments oxygen can still be detected up to \sim 20 nm along the growth direction. Most likely, this is due to the interdiffusion of oxygen atoms from the surface into the structure, assisted by the sputtering procedure. In the as-grown sample the maximum oxygen content is found at the surface. After the oxygenation treatment a peak in the oxygen content is observed at \sim 17 nm and is a factor of 2 higher than that of the oxygen on the surface of the as-grown sample. Going deeper into the sample the oxygen content drops to zero at approximately 60 nm. Such a depth profile

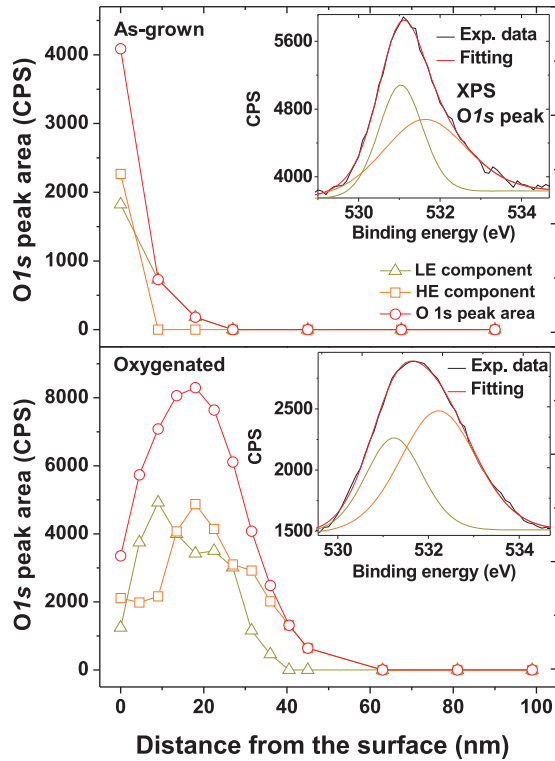


FIG. 1. (Color online) Depth profile of the oxygen $1s$ peak measured by XPS. The oxygen content in the as-grown sample (top) is maximum at the surface and vanishes at 20 nm. The oxygenated sample (bottom) has the largest oxygen content at 17 nm from the surface and it reduces to zero at approximately 60 nm. The insets display the oxygen $1s$ peak at the surface of the as-grown (top) and oxygenated (bottom) samples where two contributions at higher (squares) and lower (triangles) energies are combined in the fitting to give the total peak area.

of the oxygen content in the plasma-treated sample reflects the energy distribution of the oxygen species penetrating into the structure of the films. As already mentioned, the value of the peak oxygen content is twice as high in the treated sample as that on the surface of the as-grown sample. However, the total amount of oxygen contained in the whole sample volume expressed as the area of the depth profile curves presented in Fig. 1 [O $1s$ peak area (CPS) vs distance from the surface (nm)] is almost ten times higher after oxygenation, which accounts for the observed distinct changes in the electrical and magnetic properties of the samples after treatment.

The XPS oxygen $1s$ peaks of the as-grown and oxygenated samples at the surface of the films are displayed in the insets of Fig. 1, top and bottom, respectively. Fitting of the O $1s$ signal requires consideration of two contributions to the total area of the peak. By modeling the XPS data the higher- and lower-energy contributions can be traced in the depth profile as can be observed in Fig. 1. In the case of the as-grown sample, the high-energy peak can only be found in the vicinity of the surface while for the oxygenated sample a similar contribution from the high- and low-energy peaks is also observed inside the film in the region of highest oxygen content. The decomposition of the XPS O $1s$ in two components has already been reported in studies of oxygen adsorption on GaAs.¹³ The authors propose

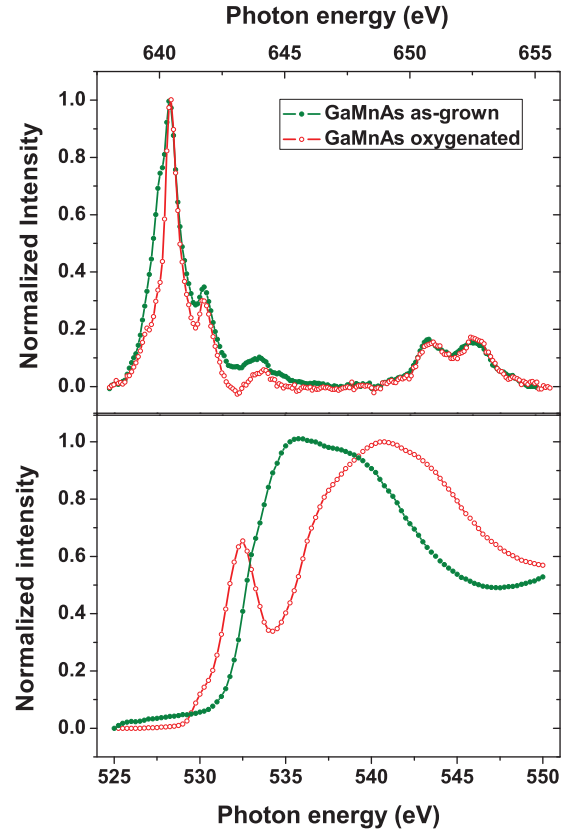


FIG. 2. (Color online) Normalized XAS spectra of the Mn $L_{2,3}$ edges (top) and the oxygen Kedge (bottom) for the as-grown (full symbols) and oxygenated (open symbols) (Ga,Mn)As samples. While the Mn d^5 electronic state is preserved upon oxygenation the type of oxygen present in the oxygenated sample is clearly different from that of the surface oxide of the as-grown sample.

that the higher-energy component may correspond to a less tightly chemisorbed type of oxygen. Additionally, the authors present evidence supporting the idea of dissociated oxygen being the species represented by the lower-energy peak. As previously mentioned both high- and low-energy contributions are comparable in the oxygen-rich parts of the oxygenated samples. In the present case the diffusion of dissociated oxygen into the structure of the films seems to be a reasonable scenario. On the other hand, (Ga,Mn)As is known to have energetically different interstitial sites. There are two inequivalent tetrahedral positions surrounded by four As or Ga atoms, respectively, and one with hexagonal symmetry. However, the tetrahedral sites are strongly preferred over the hexagonal sites by the manganese atoms in interstitial positions.¹⁴ In view of these facts, we tend to attribute the high- and low-energy contributions in the oxygenated samples to dissociated oxygen species in differently coordinated interstitial sites inside the (Ga,Mn)As lattice.

In Fig. 2 top and bottom the Mn L_2 and L_3 edges and the oxygen K edge x-ray absorption spectra (XAS) for as-grown and oxygenated film A are presented. The spectra were taken after sputtering the samples for 5 min following Ref. 15 at a rate of approximately 1 monolayer (ML)/min. In the Mn spectra no mayor differences upon oxygenation are observed apart from the reduction of the intensity of the low-energy

shoulder of the main peak at 640 eV. The decrease in intensity of this particular feature has already been observed in (Ga,Mn)As after annealing¹⁶ and therefore is unrelated to the oxygenation treatment and only accounts for a small annealing effect given the working temperature of 177 °C during plasma treatment. Taking these considerations into account, the spectra before and after the treatment show the typical line shape corresponding to the d^5 electronic state of Mn, indicating that no major changes in the electronic configuration of the Mn magnetic centers took place during oxygenation. However, such a good correspondence between the as-grown and oxygenated samples is not observed in the oxygen K edge spectra. It can be seen in Fig. 2 (bottom) that the profile changes dramatically after plasma treatment.

A similar XAS profile to the one presented in Fig. 2 (bottom) for the as-grown sample has been reported for other (Ga,Mn)As materials and has been attributed to MnO forming on the surface of GaMnAs.¹⁰ The spectrum shows a single broad structure centered approximately around 537 eV as the result of the superposition of multiple peaks with similar energy. The XAS signal corresponding to the oxygenated sample consists of a broad peak (540 eV) and a feature at lower energies (532 eV). According to studies of manganese oxides in the literature the energy range corresponding to the O K edge involves transitions from the O $1s$ level to excited levels of O $2p$ character hybridized with the Mn $3d$ and $4sp$ states at lower and higher energies, respectively. The O $2p$ -Mn $3d$ states have predominantly Mn character while the O $2p$ -Mn $4sp$ states are more related to the oxygen $2p$ orbitals.¹⁷⁻²⁰ The scenario in the present case is more complex than that of manganese oxides since in our (Ga,Mn)As samples the manganese atoms are diluted and the oxygen atoms will interact not only with the magnetic centers but also with the gallium and arsenic atoms. The Mn $L_{2,3}$ edges do not present major changes upon oxygenation; therefore in order to explain the change in the oxygen K edge spectra we assume that the oxygen measured before and after the treatment is not in the same electronic state. The change in the electronic state of the oxygen after the treatment is most likely due to a different coordination with respect to that in the MnO and As or Ga surface oxides. In addition, when considering that the incorporated oxygen present in the oxygenated samples diffuses from the plasma into the (Ga,Mn)As lattice, where it possibly exists in interstitial sites, we would intuitively argue that the species that will most easily diffuse into the material will be uncharged, namely, atomic oxygen. This last argument suggests that the incorporated oxygen might have a different oxidation state (O^0) with respect to that in the MnO surface oxide (O^{2-}). This in combination with a different coordination given by the chemical environment of the (Ga,Mn)As interstitial sites as shown earlier by XPS gives rise to the changes observed in the XAS profile.

In Fig. 3(a) the resistance vs temperature plots of as-grown and oxygenated samples are displayed. There is a clear shift of the resistance peak which indicates a decrease of the Curie temperature²¹ by about 30% from 45 to 32 K together with an increase in resistance at all temperatures. These measurements were performed on sample *B* where the thickness of the magnetic film is 40 nm. According to the depth profile presented in Fig. 1 this thickness will contain only the largest concentration of oxygen and therefore will resemble the largest effect of the

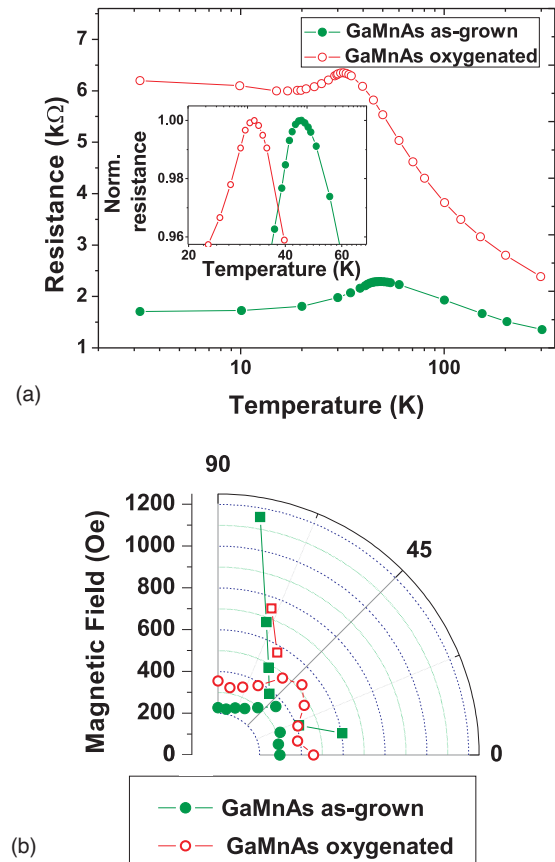


FIG. 3. (Color online) (a) Resistance vs temperature for as-grown (full symbols) and oxygenated (Ga,Mn)As (open symbols). A closeup of the resistance peaks is shown in the inset. (b) First (circles) and second (squares) switching fields as a function of the orientation of the magnetic field with respect to the $[110]$ direction at a temperature of 2 K.

plasma treatment for an oxygenation time of 3 h. The effect of oxygenation was also investigated by angle-resolved magnetotransport measurements at a temperature of 2 K. Figure 3(b) presents the dependence of the coercive field on the angle of the applied magnetic field with respect to the $[110]$ uniaxial easy axis direction²³ (perpendicular to the Hall bar longitudinal axis). A significant increase in the coercive fields in all directions is observed for the oxygenated sample with respect to the as-grown material. Studies in the literature correlate the increase in the coercive fields of (Ga,Mn)As materials to a decrease in the value of the Curie temperature and a decrease in the hole carrier density,⁶ in agreement with the results presented in Fig. 3(a). Additionally, other studies report significant changes in the coercive fields upon variations of the lattice strain induced by piezoactuators.²² Taking these facts into account, it is likely that the large amount of oxygen incorporated after the plasma treatment may contribute to the increase in the coercive fields not only by reducing the carrier density but also by inducing a moderate change in strain in the lattice.

The shape of the angular dependence of the coercive field is determined by the relative strength of the uniaxial and biaxial anisotropy components present in (Ga,Mn)As. The qualitative rectangular shape of the plot does not change after oxygenation, indicating a rather constant relation between the

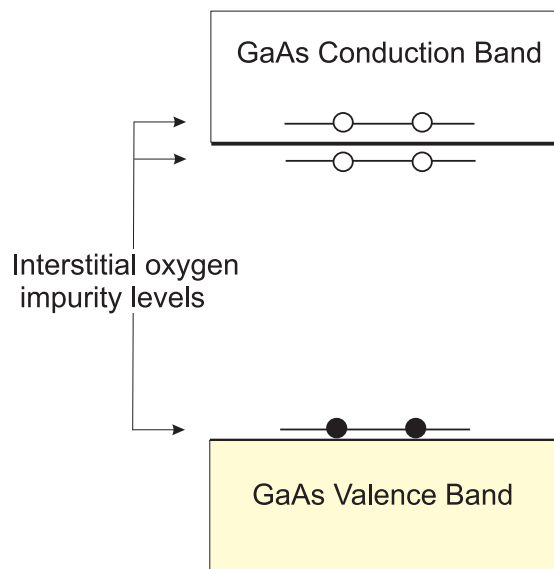


FIG. 4. (Color online) Diagram of the electronic levels introduced by a neutral oxygen impurity sitting in an interstitial site in GaAs [adapted from Orellana *et al.* (Ref. 24)].

magnetic uniaxial and cubic anisotropy energies. In particular, the ratio of approximately 1.2 between the coercive fields along the uniaxial easy axis (0° , $[110]$ direction) and the uniaxial hard axis (90° , $[1\bar{1}0]$ direction) observed for the as-grown sample is also found after the oxygenation treatment regardless of the overall increase in the values of the switching fields. Taking into account that the different contributions to the magnetic anisotropy in the system remain approximately constant after the treatment, the role of strain induced by the large amount of oxygen incorporated may be taken as negligible in the present case. As previously mentioned, the Mn L_2 and L_3 edges show the typical Mn d^5 line shape for both as-grown and oxygenated samples, indicating that the magnetic moments situated at the Mn sites can be considered constant. Keeping in mind the XAS results and the theory of hole-mediated ferromagnetism in (Ga,Mn)As, the Curie temperature shift observed upon oxygenation can be explained in terms of changes in the hole-carrier density.

It was discussed that the oxygen introduced by the treatment is thought to be neutral and possibly in interstitial positions. Theoretical studies in the literature analyzing oxygen impurities in GaAs show that neutral oxygen in interstitial sites is one of the stable configurations in pure and p - or n -doped GaAs.²⁴ These calculations show that interstitial oxygen atoms introduce fully occupied states close to the top of the valence band as shown in the diagram in Fig. 4. As introduced earlier, a decrease in charge carrier concentration is predicted to

cause a weakening of the ferromagnetic coupling which has been widely confirmed by experiments.^{25–27} Moreover, in the present case the weakening of the magnetic interaction has been shown not to be related to a loss of localized Mn moments therefore implying a hole-quenching effect, an idea supported by electrical transport measurements. Assuming that neutral oxygen in interstitial positions is a good picture of the structure of the (Ga,Mn)As samples after treatment, the weakening of the ferromagnetic coupling by hole compensation can be explained by the quenching of holes by electrons from the occupied states of the interstitial oxygen atoms that lay close to the top of the valence band.

In conclusion, we have modified the magnetic properties of (Ga,Mn)As through exposure to oxygen plasma. XAS measurements indicate that the occupation of the $3d$ levels of the Mn atoms remains unchanged upon oxygenation whereas the O K edge signal shows drastic changes with respect to the signal for the as-grown sample. Magnetotransport measurements show a significant decrease in the strength of the ferromagnetic coupling reflected in a reduction of the Curie temperature as well as an increase of the coercive fields. XAS measurements suggest that the mechanism behind the weaker ferromagnetic properties after the treatment is not related to a reduction in the local Mn magnetic moments upon oxygenation. The changes observed in the magnetic properties are related to a modulation of the hole density manifested in an increase in the zero-field resistance at all temperatures which depends on the density of the oxygen interstitial atoms. The possibility of a combined effect of hole compensation and lattice strain induced by the treatment can not be excluded given the large amount of oxygen incorporated in the system. For the present case no significant changes in the magnetic anisotropy have been observed after the treatment which indicates a negligible role of strain related effects. However, the effects of strain may have to be taken into account if larger amounts of oxygen species are incorporated. It is important to note that changes in the carrier density can also be reflected in the magnetic anisotropy, therefore, the distinction between carrier modulation and strain effects at large oxygen concentrations may not be trivial.

The oxygenation treatment of (Ga,Mn)As presented in this study can be applied to large areas of a film. Using suitable masks it can be exploited for the creation of regular and widely extended patterns of microstructures having different magnetic properties that can be relevant for practical applications.

ACKNOWLEDGMENTS

We wish to thank Alexander Bittner for valuable help with the oxygen plasma system and Sebastian Stepanow for helpful discussion.

*Present address: Institut Néel–Département Nano, Equipe Micro et Nano Magnétisme, 25 Av. des Martyrs, Bât. K, 38042 Grenoble cedex 09; liza.herreradiez@grenoble.cnrs.fr

†Present address: Instituto di Struttura della Materia, CNR, via del Foso del Cavaliere 100, 00133 Rome, Italy.

¹H. Ohno, *Science* **281**, 951 (1998).

²K. W. Edmonds, K. Y. Wang, R. P. Campion, A. C. Neumann, N. R. S. Farley, B. L. Gallagher, and C. T. Foxon, *Appl. Phys. Lett.* **81**, 4991 (2002).

³K. Y. Wang, R. P. Campion, K. W. Edmonds, M. Sawicki, T. Dietl, C. T. Foxon, and B. L. Gallagher, in *Proceedings of the 27th International Conference on Physics of Semiconductors*, edited by

- J. Menéndez and C. G. Van de Walle, AIP Conf. Proc. No. 772 (AIP, Melville, New York, 2005), p. 333.
- ⁴M. Malfait, J. Vanacken, V. V. Moshchalkov, W. Van Roy, and G. Borghs, *Appl. Phys. Lett.* **86**, 132501 (2005).
- ⁵S. T. B. Goennenwein, T. A. Wassner, H. Huebl, M. S. Brandt, J. B. Philipp, M. Opel, R. Gross, A. Koeder, W. Schoch, and A. Waag, *Phys. Rev. Lett.* **92**, 227202 (2004).
- ⁶L. Thevenard, L. Largeau, O. Mauguin, A. Lemaître, and B. Theys, *Appl. Phys. Lett.* **87**, 182506 (2005).
- ⁷T. Dietl, H. Ohno, and F. Matsukura, *Phys. Rev. B* **63**, 195205 (2001).
- ⁸[<http://www.pvateplaamerica.com>].
- ⁹L. Herrera Diez, R. K. Kremer, A. Enders, M. Rössle, E. Arac, J. Honolka, K. Kern, E. Placidi, and F. Arciprete, *Phys. Rev. B* **78**, 155310 (2008).
- ¹⁰G. S. Chang, E. Z. Kurmaev, L. D. Finkelstein, H. K. Choi, W. O. Lee, Y. D. Park, T. M. Pedersen, and A. Moewes, *J. Phys.: Condens. Matter* **19**, 076215 (2007).
- ¹¹W. Storm, D. Wolany, F. Schröder, G. Becker, B. Burkhardt, L. Wiedmann, and A. Benninghoven, *J. Vac. Sci. Technol. B* **12**, 147 (1994).
- ¹²J. T. Wolan, C. K. Mount, and G. B. Hoflund, *Appl. Phys. Lett.* **72**, 1469 (1998).
- ¹³W. Ranke, Y. R. Xing, and G. D. Shen, *Surf. Sci.* **122**, 256 (1982).
- ¹⁴J. Mašek, F. Mácá, *Phys. Rev. B* **69**, 165212 (2004).
- ¹⁵F. Maccherozzi, G. Panaccione, G. Rossi, M. Hochstrasser, M. Sperl, M. Reinwald, G. Woltersdorf, W. Wegscheider, and C. H. Back, *Phys. Rev. B* **74**, 104421 (2006).
- ¹⁶Y. Ishiwata, M. Watanabe, R. Eguchi, T. Takeuchi, Y. Harada, A. Chainani, S. Shin, T. Hayashi, Y. Hashimoto, S. Katsumoto, and Y. Iye, *Phys. Rev. B* **65**, 233201 (2002).
- ¹⁷S. Kobayashi, I. R. M. Kottegoda, Y. Uchimoto, and M. Wakihara, *J. Mater. Chem.* **14**, 1843 (2004).
- ¹⁸F. M. F. de Groot, M. Grioni, J. C. Fuggle, J. Ghijsen, G. A. Sawatzky, and H. Petersen, *Phys. Rev. B* **40**, 5715 (1989).
- ¹⁹B. Gilbert, B. H. Frazer, A. Belz, P. G. Conrad, K. H. Neilson, D. Haskel, J. C. Lang, G. Srajer, and G. De Stasio, *J. Phys. Chem. A* **107**, 2839 (2003).
- ²⁰D. M. Sherman, *Am. Mineral.* **69**, 788 (1984).
- ²¹A. Van Esch, L. Van Bockstal, J. De Boeck, G. Verbanck, A. S. van Steenbergen, P. J. Wellmann, B. Grietens, R. Bogaerts, F. Herlach, and G. Borghs, *Phys. Rev. B* **56**, 13103 (1997).
- ²²C. Bihler, M. Althammer, A. Brandlmaier, S. Geprägs, M. Weiler, M. Opel, W. Schoch, W. Limmer, R. Gross, M. S. Brandt, and S. T. B. Goennenwein, *Phys. Rev. B* **78**, 045203 (2008).
- ²³H. X. Tang, R. K. Kawakami, D. D. Awschalom, and M. L. Roukes, *Phys. Rev. Lett.* **90**, 107201 (2003).
- ²⁴W. Orellana, A. C. Ferraz, *Phys. Rev. B* **61**, 5326 (2000).
- ²⁵G. Bouzerar, T. Ziman, and J. Kudrnovsk, *Europhys. Lett.* **69**, 812 (2005).
- ²⁶Chiba, M. Sawicki, Y. Nishitani, Y. Nakatani, F. Matsukura, and H. Ohno, *Nature (London)* **455**, 515 (2008).
- ²⁷M. Sawicki, D. Chiba, A. Korbecka, Y. Nishitani, J. A. Majewski, F. Matsukura, T. Dietl, and H. Ohno, *Nature Phys.* **6**, 22 (2010).